Supplementary data for

Structure modulation of g-C_3N_4 in the TiO_2{001}/g-C_3N_4 hetero-structures for boosting photocatalytic hydrogen evolution

Qianqian Shang[a], Yuzhen Fang[a], Xingliang Yin[a] and Xiangjin Kong[a]*.

[a]College of Chemistry and Chemical Engineering, Liaocheng University, Liaocheng, 252000, China.

S1. The size distribution of TiO_2 {001} in TCN-1;

S2. The TEM image of CN-200;

S3. The size distribution of CN-QD in TCN-3;

S4. The TEM image of pure g-C_3N_4 quantum dots (CN-QDs);

S5. The magnified FT-IR spectra of samples between 3000 and 3500 cm^{-1};

S6. The size distribution of TiO_2{001} in TCN-2;

S7. The size distribution of TiO_2{001} in TCN-3;

S8. Comparison of the photocatalytic H_2 evolution activity of the prepared TCN-2 with that of photocatalysts in literature;

S9. The atomic content percent of Ti, O, C, N, F in the prepared samples;

S10. The average lifetime of charge carriers for the prepared samples;

S11. The size of (101) facets in the prepared samples calculated by the Scherrer equation.

S1. The size distribution of TiO_2 {001} in TCN-1

According to the TEM image of Fig. 2(b), the size distribution of TiO_2 {001} nanosheets in TCN-1 is shown in Fig. S1 (measured by Nano measure 1.2), and the mean diameter of the prepared TiO_2 {001} nanosheets is 18 nm.

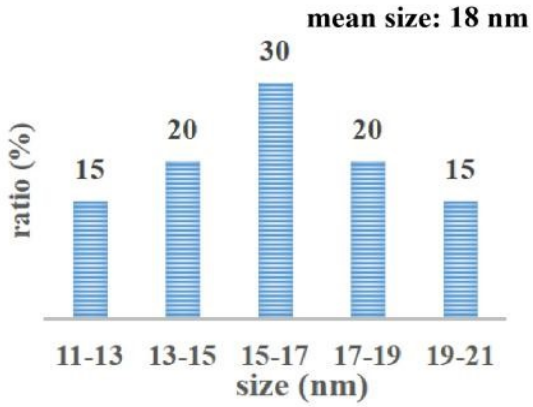

Fig. S1. The size distribution of TiO_2 {001} nanosheets in TCN-1 heterostructure.

S2. The TEM image of CN-200

To detect the effects of HF acid further, BCN was treated under the same condition with CNS-2 except without adding HF acid, the obtained sample was named as CN-200. It is apparent in Fig. S2 that the obtained CN-200 shows a typical layered structure with a large area.

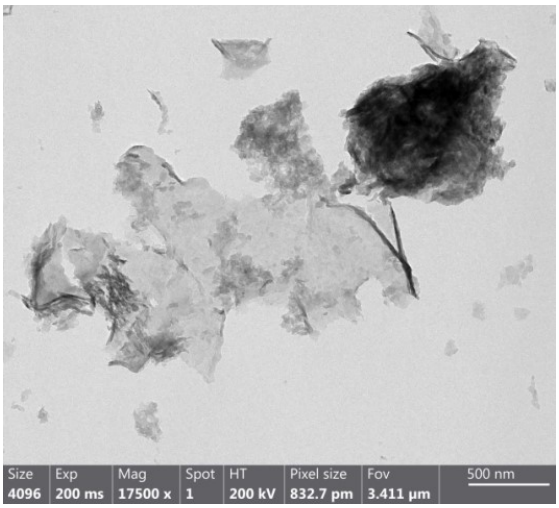

Fig. S2. The TEM image of CN-200 prepared at the same condition with CNS-2 except without adding HF acid.

S3. The size distribution of CN-QDs in TCN-3

According to the TEM image of Fig. 3(b), the size distribution of CN-QDs in TCN-3 is shown in Fig. S3(measured by Nanomeasure 1.2) and the mean diameter of the prepared CN-QDs is 3 nm.

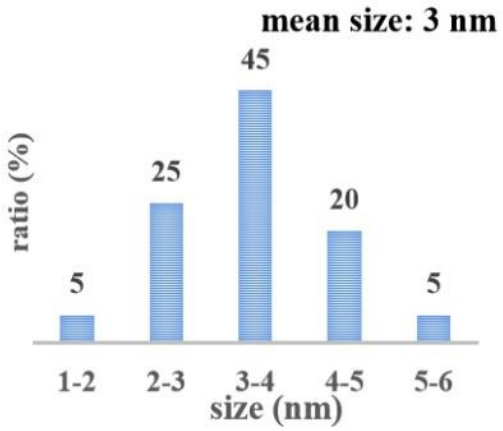

Fig. S3. The size distribution of CN-QD in TCN-3 heterostructure.

S4. The TEM image of pure g-C_3N_4 quantum dots (CN-QDs)

As shown in Fig. S4, the pure CN-QDs has been synthesized at the same condition with TCN-3 except without adding the TBOT molecules.

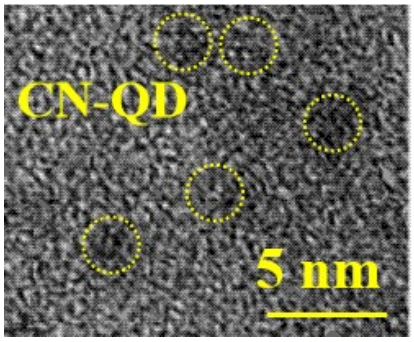

Fig. S4. The TEM image of pure g-C_3N_4 quantum dots (CN-QDs) prepared at the same condition with TCN-3 except without adding the TBOT molecules.

S5. The magnified FT-IR spectra of samples between 3000 and 3500 cm^{-1}

According to magnified FT-IR spectra of samples between 3000 and 3500 cm^{-1} (shown in Fig. S5), the intensity of the characteristic vibration peaks between 3000 and 3500 cm^{-1} increases with the increasing of the synthetic temperature. The increased exposure of N-H group could be attributed to the increased break extent of C-N chemical bonds between the adjacent tri-s-triazine units under the enhanced synthetic temperature.

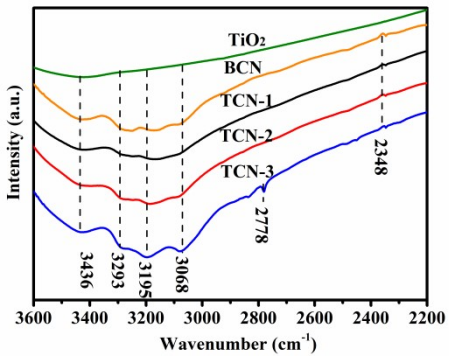

Fig. S5. The magnified FT-IR of prepared samples between 3000 and 3500 cm^{-1}.

S6. The size distribution of TiO_2{001} in TCN-2

According to the TEM image of Fig. 3(b), the size distribution of TiO_2{001} nanosheets in TCN-2 is shown in Fig. S6 (measured by Nano measure 1.2), and the mean diameter of the prepared TiO_2{001} nanosheets in TCN-2 is 20 nm.

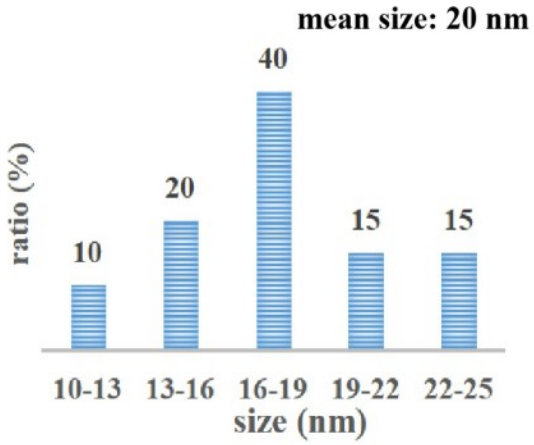

Fig. S6. The size distribution of TiO_2{001} nanosheets in TCN-2 heterostructure.

S7. The size distribution of TiO_2{001} in TCN-3

According to the TEM image of Fig. 4(a), the size distribution of TiO_2 {001} nanosheets in TCN-3 is shown in Fig. S7 (measured by Nano measure 1.2), and the mean diameter of the prepared TiO_2 {001} nanosheets in TCN-3 is 23 nm.

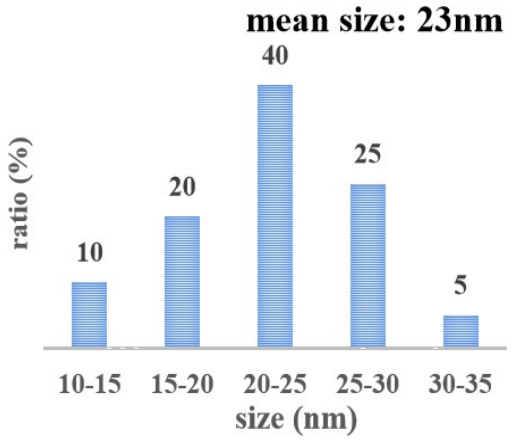

Fig. S7. The size distribution of TiO_2{001} nanosheets in TCN-3 heterostructure.

S8. Comparison of the photocatalytic H_2 evolution activity of the prepared TCN-2 with that of photocatalysts in literature

We also made a detailed comparison of the photocatalytic H_2 evolution activity of the prepared TCN with that of the photocatalysts prepared by other groups (shown in supporting information S8). Through extensive literature research, the intensify and wavelength of incident light, the distance between light source and reactor, and the addition amount of the co-catalyst are almost different, those are listed as follows (shown in Table. S1). Tan *et al.* synthesized the 3D/2D direct Z-scheme heterojunctions of hierarchical TiO_2 microflowers/g-C_3N_4 nanosheets (TiO_2/g-C_3N_4), and its photocatalytic activity of H_2 evolution was measured under the same condition with that of TCN-2 [16]. It is obvious that the prepared TCN-2 also exhibits an excellent activity of H_2 evolution than the TiO_2/g-C_3N_4 prepared by Tan group.

Table. S1 Comparison of the photocatalytic H_2 evolution activity of the prepared TCN-2 with that of photocatalysts in literature

	Cocatalyst	Light source	Highest activity ($mmol \cdot h^{-1} \cdot g^{-1}$)	Ref.
TiO_2/g-C_3N_4	Pt (3 wt%.)	$\lambda > 420$ nm	0.513	[16]
Ti^{3+}-TiO_2/g-C_3N_4	Pt (1 wt%.)	$\lambda > 420$ nm	0.287	[59]
TiO_2@g-C_3N_4	no	AM 1.5	0.0079	[60]
C-dot/g-C_3N_4/TiO_2	no	350W Xe lamp	0.01	[61]

S9. The atomic content percent of Ti, O, C, N, F in the prepared samples

Table. S2 shows the atomic content percent of Ti, O, C, N, F in the prepared samples measured by XPS. It is apparent in Table S2 that the content ratio of g-C_3N_4 in the prepared TCN heterostructures decreases with the increased of the synthetic temperature.

Table. **S2** The atomic content percent of Ti, O, C, N, F in the prepared samples

	Ti2p	O1s	C1s	N1s	F1s
TCN-1	8.92	17.55	30.45	36.96	6.12
TCN-2	10.04	18.98	28.86	35.05	7.07
TCN-3	10.69	22.66	24.7	34.4	7.55

S10. The average lifetime of charge carriers for the prepared samples.

The curves of time-resolved photoluminescence decay spectra in Fig. 10 (b) were fitted with the ExpDec2 (using the Origin software), respectively, and the obtained A_1, t_1, A_2, t_2 are shown in Table. S3. The average lifetime of charge carriers for the prepared samples was calculated according to the equation as follows, and the results are summarized in Table S3.

$$\tau_{ave} = \frac{A_1 * t_1^2 + A_2 * t_2^2}{A_1 * t_1 + A_2 * t_2}$$

Table. S3 The average lifetime of charge carriers for the prepared samples.

Samples	TiO_2	BCN	TCN-1	TCN-2	TCN-3
A_1	1928.296	42.13017	39.43025	30.17187	31.94815
t_1	1.13401	15.21908	18.08065	22.61286	19.86034
A_2	-957.757	1043.979	1085.576	1092.91	1056.961
t_2	0.46347	1.24002	1.41067	1.48712	1.33039
Lifetime (ns)	1.305	5.870	6.706	7.733	7.092

S11. The size of (101) facets in the prepared samples calculated by the Scherrer equation.

The FWHM of TiO_2 (101) facet in the prepared TCN-1, TCN-2 and TCN-3 heterostructures were measured to be 0.89^o, 0.75^o and 0.63^o, respectively. And the sizes of (101) facets in the TCN-1, TCN-2 and TCN-3 heterostructures could be calculated by the Scherrer equation:

$$D = 0.89 \lambda / (B * \cos\theta)$$

(D is the size of the specific plane, the unit is nm; λ is the wavelength of the incident wave, 0.154056 nm; B is the FWHM, the unit is rad; θ is the angle of incidence).

According to the above equation, the size of (101) facets in the prepared TCN-1, TCN-2 and TCN-3 are 8.06 nm, 9.07 nm and 10.74 nm, respectively. Therefore, the size of (101) facets in the prepared samples increases with the increase of the synthetic temperature. And this tendency is consistent with the results of TEM images.